Electric Power Systems Research 238 (2025) 111088

Contents lists available at ScienceDirect

Electric Power Systems Research

journal homepage: www.elsevier.com/locate/epsr

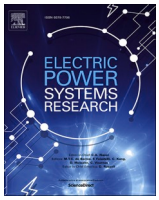

Optimal sizing of islanded microgrid using pelican optimization algorithm for Kutubdia Island of Bangladesh

Abidur Rahman Sagor [a], Md. Rifat Hazari [a], Shameem Ahmad [a], Emanuele Ogliari [c,*], Chowdhury Akram Hossain [b], Effat Jahan [a], Mohammad Abdul Mannan [a]

[a] Department of Electrical and Electronic Engineering, American International University-Bangladesh (AIUB), Dhaka 1229, Bangladesh
[b] Department of Computer Engineering, American International University-Bangladesh, Dhaka 1229, Bangladesh
[c] Department of Energy, Politecnico di Milano, Via Giuseppe La Masa, 34, 20156 Milano, Italy

ARTICLE INFO

Keywords:
Cost of energy
Island microgrid
Life cycle cost
Pelican optimization algorithm
Renewable energy source

ABSTRACT

This study proposes an optimal design approach, based on the Pelican Optimization Algorithm (POA), to configure the optimal sizing of design variables on an islanded microgrid: photovoltaic (PV) modules, wind turbines (WT), diesel generators (DG), and batteries in Kutubdia, Bangladesh based on optimal life cycle cost (LCC) and cost of energy (COE). Additionally, the economic analysis of three independent battery technologies, notably lead acid, lithium-ion, and nickel-iron are carried out to find the economically feasible technology, to ensure uninterrupted power supply. Moreover, reliability and sensitivity analyses of the optimized microgrid using POA were conducted for various reliability indices and variable interest rates. Results show that proposed POA method provides the optimal island microgrid configuration with lead acid (LA) batteries (PV/WT/LA/DG) based on a minimum LCC of $8334901, COE of 0.1080$/KWh and greenhouse gas emission amount of 19664 kgs/year. Furthermore, the outcomes generated by the POA are compared with genetic algorithm, particle swarm optimization, moth flame optimization algorithm, whale optimization algorithm and grey wolf optimization. It is found that POA method achieves more competitive results compared to other optimization techniques due to its ability to adjust parameters, fast convergence speed, and straightforward computations.

1. Introduction

Microgrids, also known as micro-energy networks, have become increasingly popular as a method to address the significant rise in consumption of electricity [1–4]. Integrating microgrids with existing electrical networks offers several advantages because they can handle specific local electricity demands, either in isolation or in combination with the utility grid. Oftentimes, these networks lack distinct financial obligations and do not require advanced technical expertise to operate [5]. Self-sufficiency in meeting load requirements in isolated microgrids is essential because of the independent generation, transmission, control, and distribution of power within these small-scale power systems [6,7]. Implementing a techno-economic solution for providing electricity to rural areas necessitates the use of a renewable energy system. Currently, it is widely believed that small-scale distributed renewable generation technologies are crucial for addressing energy-related problems [8]. Furthermore, the integration of microgrids with battery storage systems, demand response, and other conventional generation methods can mitigate the unpredictable nature of renewable energy sources (RESs), such as solar and wind power [9,10].

Optimal sizing of the microgrid is necessary to ensure that the microgrid system meets the necessary performance criteria while minimizing the system's total cost [11], optimal sizing is required. The purpose of microgrid optimal sizing is to determine the best combination of component quantity and size to achieve the desired levels of resilience, cost-effectiveness, and dependability [12]. The lack of a main grid in isolated microgrids makes optimal sizing particularly crucial for ensuring a consistent power supply [13,14]. Numerous researchers have tackled optimization problems using different techno-economic analyses, classical techniques, commercial software, and optimization algorithms to determine the optimal sizing of microgrid systems. Classical techniques have several limitations, including inflexibility, challenges in identifying a global optimum, and difficulties in adapting to dynamic changes. When it comes to handling various objectives, commercial software tools have restrictions and lack advanced optimization capabilities. Optimization algorithm techniques overcome the limitations of

* Correspondence author at: Department of Energy, Politecnico di Milano, Via Giuseppe La Masa, 34, 20156 Milano, Italy.
E-mail address: emanuelegiovanni.ogliari@polimi.it (E. Ogliari).

https://doi.org/10.1016/j.epsr.2024.111088
Received 23 May 2024; Received in revised form 19 August 2024; Accepted 15 September 2024
Available online 23 September 2024

classical techniques and commercial software tools by providing a globally optimal solution with a fast convergence speed. Algorithm outcomes provide greater efficiency in resolving complex problems [15, 16].

Different types of optimization algorithms have been proposed in the literature to solve the optimal sizing issue of microgrid systems. For instance, Alturki, F.A., et al. [17] used a genetic algorithm (GA) to minimize the annualized system cost. However, it needs to include the life cycle cost (LCC) and cost of energy (COE) while also addressing the issue of GA optimization, which tends to rapidly converge and get trapped in a locally optimal solution. Mohammed, A.Q., et al. [18] minimize the total system cost and total emission through particle swarm optimization. However, there is a need to consider LCC while addressing the PSO issues, which exhibit early convergence and become stuck in local optima. Bandopadhyay, J., et al. [19] used the moth flame optimization algorithm (MFOA) to minimize the price of electrical energy. However, it is necessary to address LCC, while MFOA issues such as limited population variety and premature convergence fall into local optima. Abo-Elyousr & Elnozahy [20] employed ant colony optimization (ACO) to minimize the net present cost, levelized cost of energy, and greenhouse gas emissions. However, it is necessary to consider LCC while addressing the ACO issue, as improper parameter setups can rapidly ignore a high-quality solution. Geleta, D.K., et al. [21] utilized the artificial bee colony (ABC) algorithm to minimize the total annual cost. Nevertheless, it is necessary to consider LCC while addressing ABC algorithm issues such as accuracy requirements, premature convergence, and additional processing demands. Diab, A.A.Z., et al. [22] used the whale optimization algorithm (WOA) to minimize the cost of energy. However, it needs to include the LCC while also addressing the WOA issues, which exhibit a slow convergence rate and limited accuracy. Al-Shamma'a, A.A., et al. [23] employed the grasshopper optimization algorithm (GOA) to minimize the annual system cost. However, it needs to include the LCC while also addressing GOA issues, as an optimal solution requires a large number of iterations. Sanajaoba, S., et al. [24] used the firefly optimization algorithm (FOA) to minimize the cost of energy. However, it needs to consider LCC while also addressing FOA issues, the optimal solution of which entails challenges in local searches and a high convergence rate. Kaur, R., et al. [25] utilized grey wolf optimization (GWO) to minimize the levelized cost of energy. Yet, it needs to be considered LCC while also addressing the GWO issues, which prevent local search from existing because of the slow convergence speed in the later stages of the iteration. Cetinbas, I., et al. [26] used harris hawks optimization (HHO) to minimize the cost of energy. However, it needs to include the LCC while also addressing the HHO issues; the imbalance between its exploration and exploitation capabilities quickly converges, and it becomes stuck in local optima. Kumar,P. P., et al. [27] used the salp swarm algorithm (SSA) to minimize the annual levelized cost and levelized cost of energy. However, there is a need to consider LCC while also addressing issues with SSA, such as ineffective exploration and exploitation, a slow convergence rate, and inadequate exploitation. Sallam, M. E., et al. [28] used the turbulent flow of water (TFW) algorithm to minimize the annual system cost and carbon dioxide emissions. However, it needs to consider LCC while also addressing TFW algorithm issues, eliminating control parameter

Table 1
Summaries of related studies on optimal sizing of microgrid.

Ref.	Sources used in microgrid	Optimization Technique	Objective Function	Application & Sizing	Constraints	Limitations	Issues of optimization techniques
[17]	PV, WT, DG, BESS	GA	Minimize the annualized system cost	Residential Area & Installed 456kW	Reliability: Loss of power supply probability (LPSP)	LCC and COE are not taken into account.	GA converges quickly and gets stuck in the local optimal solution of a complex problem.
[18]	PV, DG, BESS	PSO	Minimize the total system cost and total emission	Residential Area & Installed 250kW	Reliability: Continuous supply of the load demand	LCC are not taken into consideration	The PSO algorithm shows early convergence and becomes caught in local optima when used for complex problems.
[19]	PV, WT, DG, BESS	MFOA	Minimize the price of electrical energy	Residential Area, Installed 50 kW and 15 households	Reliability: LPSP	LCC are not taken into account.	Issues such as limited population variety fall into local optima and premature convergence.
[20]	PV, WT, DG, Biomass BESS	ACO	Minimize the net present cost, levelized cost of energy and greenhouse gases emissions	Rural area & Installed 100kW	Reliability: LPSP Energy resources installation limit	LCC are not taken into consideration.	Setting parameters is a complex process, and improper parameter setting makes it simple to ignore a high-quality solution.
[22]	PV, WT, DG, BESS	WOA	Minimize the cost of energy	Residential Area & Installed 400kW	Reliability: LPSP	LCC is not being considered.	WOA exhibits a slow convergence rate and limited accuracy.
[23]	PV, WT, DG, BESS	GOA	Minimize the annual system cost	Rural Area & Installed 1 MW	Reliability: LPSP, renewable energy factor, PV, WT, DG & Battery power limit	LCC are not being considered.	The computation requires large stages.
[24]	WT, PV, BESS	FOA	Minimize the cost of energy	Rural Area & Installed 100kW	Reliability: Loss of load probability (LOLP) Limit the generations	LCC are not taken into account.	The algorithm may encounter difficulties in local search and exhibit a rather lengthy convergence time.
[25]	PV, WT, BESS	GWO	Minimize the levelized cost of energy	Rural Area & Installed 10kW	Reliability: LPSP, excess energy generation (EEG)	LCC is not taken into consideration.	Lack of ability to exist local search due to slow convergence speed at the later part of the iteration. It needs to improve in precision and accuracy.
[26]	PV, WT, DG, BESS	HHO	Minimize the cost of energy	Campus & Installed 500kW	Reliability: LPSP	There is no consideration of LCC.	The early convergence of HHO occurs when there is an imbalance between its exploration and exploitation capabilities, leading to the algorithm getting stuck in local optima.

Here, PV, WT, DG and BESS stands for photovoltaic, wind turbine, diesel generator and battery energy storage system respectively.

Fig. 1. The study area location is on the map. (Source: Google maps).

selection, and increasing the convergence rate. Yang, D., et al. [29] utilized teaching learning-based optimization (TLBO) to minimize the total annual cost. However, it is necessary to consider LCC while also addressing TLBO issues that arise from weak exploration, so it has poor performance for solving complex optimization problems and capturing the global optimal solution in a smaller number of function evaluations. Khan, A., et al. [30] used jaya learning-based optimization (JLBO) to minimize the total annual cost. However, it needs to consider LCC while also addressing the JLBO issues that arise from premature convergence and local optima trapping. Cai, W., et al. [31] used gorilla troops optimization (GTO) to minimize the cost of energy and the net present cost. However, it is necessary to consider LCC while addressing GTO issues such as the imbalance between exploration and exploitation and its slow convergence rate. Table 1 displays the summary of related studies on optimal microgrid sizing along with their limitations.

From the aforementioned studies, it can be observed that even though life cycle cost (LCC) is the most crucial factor of the microgrid systems to evaluate the life cycle of equipment, this factor has not been considered in the above study. LCC is a method for evaluating costs over a specific period, taking into account all relevant economic factors, such as capital expenses and future operational costs [32]. This methodology enables the quantification of costs and benefits, facilitating the comparison of different solutions using a consistent economic standard. It achieves this by discounting all future costs and benefits by a specified reference year. Although the LCC methodology relies on estimating and evaluating future events and their unpredictable outcomes, it provides a thorough and inclusive method for evaluating and comparing different investment opportunities [33]. Furthermore, the optimization techniques used for optimal sizing of microgrids also possess drawbacks (rapid or premature convergence, improper parameter setting, computational complexity, etc.), which are presented in Table 1. To overcome the shortcomings of the previously used optimization algorithms for microgrid sizing, in this study, a pelican optimization algorithm (POA) is proposed for microgrid optimal sizing considering LCC and cost of

Table 2
Load profile of the case study area [35].

SL.	Load Types		Appliances	Rated Power (W)	Quantity	Toal Entities	Total Load (kW)
1	Household load	High income	Light	40	6	500	120
			Fan	70	3		105
			Fridge	20	1		10
			TV	80	1		40
			Washing Machine	500	1		250
			Motor-Pump	1000	1		500
		Middle income	Light	40	3	1000	120
			TV	70	2		140
			Fan	20	1		20
		Low income	Light	40	2	500	40
			Fan	70	1		35
2	Residential hotel and resort		Light	40	50	10	20
			Fan	70	20		14
			Motor-Pump	20	10		2
			TV	2000	2		40
3	Educational Institutes		Light	40	10	10	20
			Fan	70	5		14
			Motor-Pump	2000	1		40
4	Super-shops		Light	40	10	10	4
			Fan	70	5		3.5
			Motor-Pump	1000	1		10
			TV	20	1		0.2
5	Motor-pump		Light	40	100	1	4
			Fan	70	20		1.4
			Fridge	20	1		1
			Motor-Pump	1000	1		5
6	Factory makes ice			10,000	1	1	10
7	Charging station for EV			5000	1	1	5
Total demand							1574.1

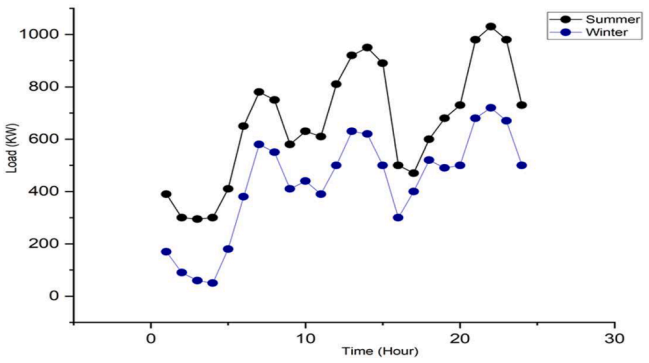

Fig. 2. Daily load profile for summer and winter seasons.

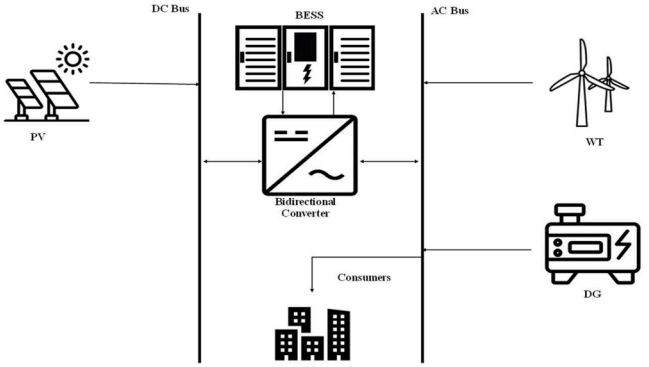

Fig. 3. Proposed microgrid.

energy (COE). The benefits of POA include the ability to adjust parameters, fast convergence speed, and straightforward computations. The POA technique outperforms existing techniques by efficiently balancing the exploration and exploitation phases, resulting in better and more competitive performance. It offers a population-based method via an iterative process that converges to nearly the optimal solution [34,48]. Incorporating LCC calculations during the computing process improves an island microgrid's techno-economic analysis. The contributions of the study are as follows:

- Pelican optimization algorithm (POA) is used to determine the optimal configuration of microgrid that minimizes life cycle costs (LCC) and cost of energy (COE), satisfies demand, and ensures a loss of power supply probability (LPSP).
- Determine the most cost-effective and sustainable options for storing energy in a microgrid, focusing on photovoltaic (PV), wind turbine (WT), diesel generator (DG), and battery technologies, especially lead acid (LA), lithium-ion (Li-ion), and nickel-iron (Ni-Fe).
- The effect of different reliability index (LPSP) constraints is presented to confirm the reliability of the proposed approach for minimization of LCC and COE.
- A sensitivity study is conducted to determine how designed variables affect LCC, COE, and CO_2 emission.

The following sections are structured: Section 2 details the case study area. Section 3 provides a detailed explanation of the microgrid modelling. The mathematical formulation model is presented in Section 4. The use of the POA to solve the problem is explained in Section 5. The results and discussions are shown in Section 6. The conclusion is presented in Section 7.

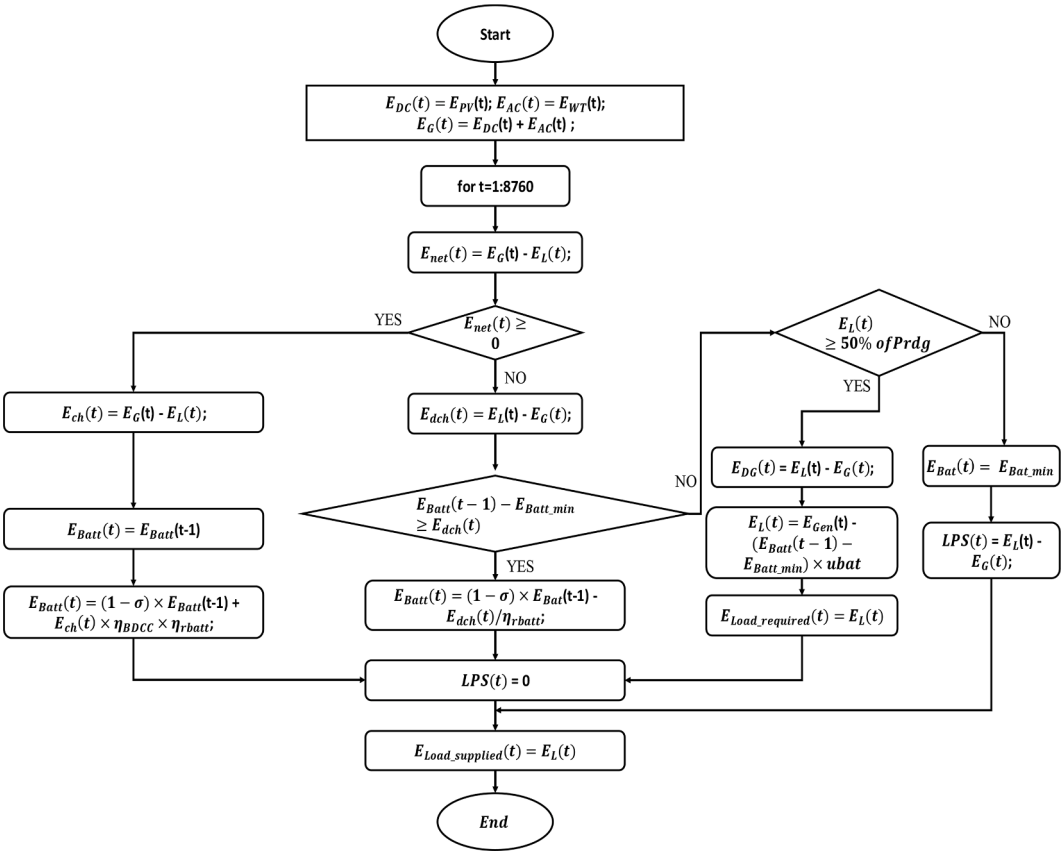

Fig. 4. Energy management strategy (EMS) of the proposed microgrid.

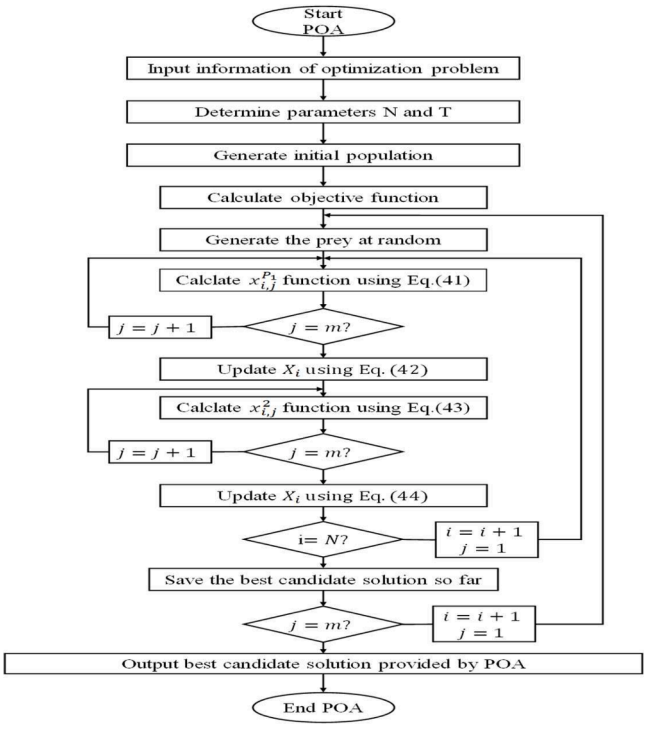

Fig. 5. Flowchart of POA.

2. Case study: Kutubdia island, Bangladesh

The Kutubdia is an upazila in the Chittagong division of the Cox's Bazar district in Bangladesh. In 1983, the island was elevated to the status of upazila. Kutubdia covers a length of 18 miles (29 km), a width of 2 miles (3.2 km), and an area of 36 m^2iles (93 km^2). The coordinates of Kutubdia are 21.8167°N 91.8583°E. The municipality comprises 58,463 households and covers 215.79 km^2s (83.3 m^2iles). Sea level rise and climate change face a hazard of submerging the island in the Bay of Bengal. Fig. 1 displays a satellite view of the site provided by Google Maps.

Connected loads for Kutubdia Island include a community of 2000 households, 10 hotels and resorts, 10 educational institutions, 10 supermarkets, one hospital, one ice plant, and one electric vehicle (EV) charging station. Table 2 represents the specific information on load categories, equipment ratings, quantity, and other relevant factors. Households are classified into high-, middle-, and low-income categories based on their level of consumption. A high-income individual's household domestic load comprises a water pump, lamp, fan, television, and refrigerator. Both a washing machine and a water pump are absent from middle-class households. The educational institute's load demand occurs from 8:00 – 17:00 hours. The supermarkets operate from early morning till midnight. The primary electrical loads in the shop area are the light fittings, fans, and motors. The medical facility must maintain a constant connection as a vital load to ensure the provision of emergency services. Additionally, during all days of the week, the ice-making facility is in continuous operation, as fishing is the primary occupation of the people who live on the island. The expected load indicates the existence of two distinct seasons: winter, which occurs between November to February, and summer, which occurs between March to October. Fig. 2 illustrates the load profile of two seasons based on the expected load consumption of the island area. During both seasons, the highest level of demand occurs between 21:00 and 23:00 [35].

3. Proposed microgrid modelling

During the optimal sizing procedure of microgrids, it is essential to have accurate mathematical models of their components. The study presented a microgrid that integrates PV and WT energy sources, together with a backup system comprising a DG and BESS. The schematic diagram of the proposed microgrid is depicted in Fig. 3, with detailed descriptions of the component models provided below.

The operational energy management strategy (EMS) for the proposed microgrid is depicted in Fig. 4 and detailed as follows:

- The primary source is PV & WT, which can satisfy the load demands.
- The battery is used when PV & WT cannot satisfy the load demands.
- When BESS is empty, the DG system runs on 50% of its nominal power.

3.1. PV power generation

The PV output power can be mathematically represented as [36]:

$$P_{PV}(t) = PV_{rated} \times \left(\frac{G_t}{G_{ref}}\right) \times \left[1 + K_T \times (T_c - T_{ref})\right] \quad (1)$$

Where G_{ref} and G(t) denotes the reference solar irradiation with a value of 1000 w/m^2 and hourly solar irradiation. K_T denotes the maximum power temperature coefficient, with a value of $3.7 \times 10^{-3}(1/^{\circ}C)$. T_{ref} indicates the reference PV cell temperature, with a value of 25°C. PV_{rated} represents the PV rated power.

The following equation determines the cell temperature (T_c):

$$T_c = T_{amb}(t) + (0.0256 \times G(t)) \quad (2)$$

Where $T_{amb}(t)$ represent the hourly ambient temperature.

The energy generation of PV panel (E_{PV}) is as follows:

$$E_{PV}(t) = N_{PV} \times P_{PV}(t) \times \Delta t \quad (3)$$

Where N_{PV} represent the number of PV panel and Δt represent the is the time period and its considered 1 h.

3.2. Wind power generation

The wind power generation can be calculated as follows [36]:

$$P_{WT}(t) = \begin{cases} 0 \; V(t) \le V_{cin} \; and \; V(t) \ge V_{cout} \\ P_r^w \; V_{rat} \le V(t) \le V_{cout} \\ P_r^w \dfrac{V(t) - V_{cin}}{V_{rat} - V_{cin}} \; V_{rat} \le V(t) \le V_{cout} \end{cases} \quad (4)$$

Where P_r^w represents the WT rated power, V_{cin} denotes the cut-in speed, V_{cout} denotes the cut-out speed, V_{rat} represents the rated wind speed and V(t) denotes the intended reference height for the wind speed.

$$V(t) = V_r(t)\left(\frac{H_{WT}}{H_r}\right)^{\lambda} \quad (5)$$

Where V(t) represents the wind speed at a specific height. The wind speed at the reference height is denoted as $V_r(t)$ and the friction coefficient, λ, usually equals 1/7 for a smooth surface.

3.3. Battery energy storage system (BESS)

The following equation is utilized to determine at a specific hour t, how much energy can be stored in the battery bank [36]:

$$E_{Batt}(t) = (1 - \sigma) \times E_{Batt}(t-1) + \left(E_G(t) - \frac{E_L(t)}{\eta_{Conv}}\right) \times \eta_{CC} \times \eta_{rbatt} \quad (6)$$

Where η_{rbatt}, η_{cc}, η_{conv} & σ represent efficiency of the battery's round-trip, charge controller, converter and hourly self-discharge rate, respectively.

The equations used for electrical energy generation are as follows:

$$E_G(t) = [E_{DC}(t) + E_{AC}] \times \eta_{Conv} \quad (7)$$

$$E_{DC}(t) = E_{PV}(t) \quad (8)$$

$$E_{AC}(t) = E_{WT}(t) \quad (9)$$

When Electrical power generation is not meet the demand by RESs, the battery energy system provides the required load, which can be calculated follow as:

$$E_{Batt}(t) = (1-\sigma) \times E_{Batt}(t-1) + \left(\frac{E_L(t)}{\eta_{Conv}} - E_G(t)\right) \Big/ \eta_{rbatt} \quad (10)$$

3.4. Diesel generator (DG)

The linear law of DG hourly fuel consumption, which is determined by the amount needed to satisfy demand, can be calculated as follows [36]:

$$F_{DG}(t) = \left(a_{DG} \times P_{DG,gen}(t) + b_{DG} \times P_{DG,rat}\right) l/h \quad (11)$$

Where b_{DG} and a_{DG} represent coefficients of DG consumption curve and their respective values are $b_{DG} = 0.08414$ (l/KWh) and $a_{DG} = 0.246$ (l/KWh).

DG total annual fuel consumption in liters (TAFCIL) is calculated using the following equation:

$$TAFCIL = \sum_{t=1}^{8760} F_{DG}(t) \quad (12)$$

3.5. CO_2 emission

The expected CO_2 emissions are determined by the estimated fuel consumption per hour, which is as follows [37]:

$$CO_2 = SE_{CO_2}(kg/l) \times F_{DG}(t)\left(\frac{l}{h}\right) \quad (13)$$

Where SE_{CO_2} represent the per liter diesel's specific emission, and its value is 2.7 kg/l.

The estimation of the DG's total annual CO_2 emissions is as follows:

$$TA_{CO_2} = \sum_{t=1}^{8760} CO_2(t) \quad (14)$$

3.6. Bi-directional with a charge controller (BDC-CC)

When converting electrical energy, the BDC-CC is both a rectifier and an inverter. In rectifier mode, AC is transformed into DC; in inverter mode, DC is converted back into AC. The charge controller is advantageous by preventing the battery bank from being overcharged or discharged excessively. The calculation for determining the power rating of the BDC-CC ($P_{BDC\text{-}CC}$) is as follows [38]:

$$P_{BDC-CC} = E_{T,max} \times 1.1 \quad (15)$$

Where $E_{T,max}$ represents the highest amount of energy that can be transferred by the converter. The multiplication factor of 1.1 indicates that the converter can handle an additional 10 % of its maximum capacity.

3.7. Economic analysis

The LCC of the complete system is calculated by summing up the following costs: initial capital costs (ICC), erection cost (EREC), the present value of yearly O&M ($P_{V,O\&M}$) costs, the present value of replacement ($P_{V,REP}$) costs, and the present value of fuel ($P_{V,FUEL}$) costs [39].

$$LCC = ICC + EREC + P_{V,O\&M} + P_{V,REP} + P_{V,FUEL} \quad (16)$$

The following equation will be employed to calculate the Initial Capital Costs (ICC) of the microgrid components:

$$ICC = \left[\left(N_{PV} \times C_{PV,cap}\right) + \left(N_{WT} \times C_{WT,cap}\right) + \left(N_{BATT} \times C_{BATT,cap}\right) + \left(C_{BDC-CC,cap}\right) + \left(C_{DG,cap}\right) \right] \quad (17)$$

Where N_{PV}, N_{WT}, N_{BATT}, $C_{PV,cap}$, $C_{WT,cap}$, $C_{BATT,cap}$, $C_{BDC\text{-}CC,cap}$ and $C_{DG,cap}$ represent the no.of PV panel, WT, batteries(BATT), initial capital costs of PV, WT, BATT, BDC-CC and DG.

For microgrid component erection costs (EREC), the following equation is followed:

```
Start POA
Initialize POA
Initialize the optimization problem information
Compute the POA population size (N) and the number of iterations (T)
Location initialization of pelicans and compute the objective function
For t = 1:T
    Create the prey location at random
  For I = 1:N
        Phase 1: Moving towards prey (exploration phase)
      For j = 1:m
          Calculate new status of the jth dimension using Equation (41)
      End
      Update the ith population member using Equation (42)
      Phase 2: Winging on the water surface (exploitation phase)
        For j = 1: m
            Calculate new status of the jth dimension using Equation (43)
        End
        Update the ith population member using Equation (44)
      End
      Update best candidate solution
End
Save the best candidate solutions obtained by POA
End POA
```

Fig. 6. Pseudocode of POA.

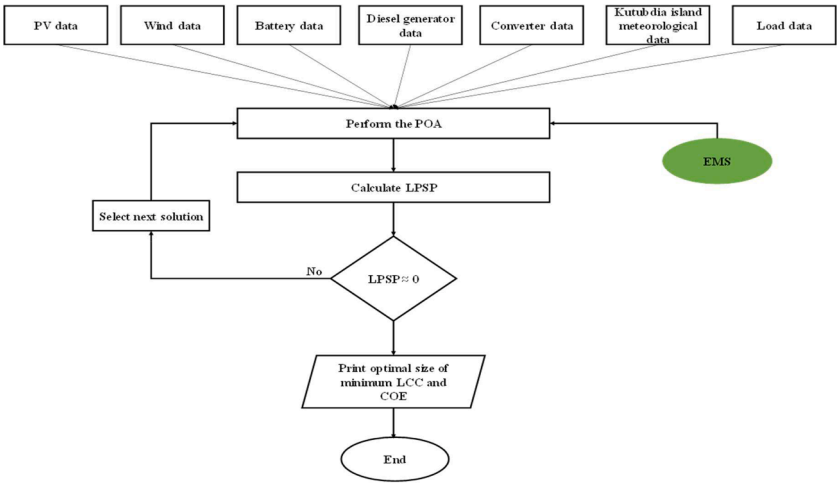

Fig. 7. Proposed optimization approach using POA.

$$EREC = \left(N_{PV} \times C_{PV,erec}\right) + \left(N_{WT} \times C_{WT,erec}\right) + \left(N_{BATT} \times C_{BATT,erec}\right) \times \sum_{b=1}^{N_r} \frac{(1+x)^{bN_c-1}}{(1+y)^{bN_c}} + \left(C_{BDC-CC,erec} \times \sum_{b=1}^{N_r} \frac{(1+x)^{bN_c-1}}{(1+y)^{bN_c}}\right) + \left(C_{DG,erec} \times \sum_{b=1}^{N_r} \frac{(1+x)^{bN_c-1}}{(1+y)^{bN_c}}\right) \tag{18}$$

Where $C_{PV,erec}$, $C_{WT,erec}$, $C_{BATT,erec}$, $C_{BDC\text{-}CC,erec}$ and $C_{DG,erec}$ represent the erection costs of PV, WT, BATT, BDC-CC and DG.

Following this, the present value of the microgrid components' annual O&M costs is calculated:

$$P_{V,O\&M} = \left[\left(N_{PV} \times C_{PV,O\&M}\right) + \left(N_{WT} \times C_{WT,O\&M}\right) + \left(N_{BATT} \times C_{BATT,O\&M}\right) + \left(C_{BDC-CC,O\&M}\right) + \left(C_{DG,O\&M}\right)\right] \times \sum_{i=1}^{N} \frac{(1+x)^{i-1}}{(1+y)^{i}} \tag{19}$$

Where $C_{PV,O\&M}$, $C_{WT,O\&M}$, $C_{BATT,O\&M}$, $C_{BDC\text{-}CC,O\&M}$ and $C_{DG,O\&M}$ represent the operation and maintenance costs of PV, WT, BATT, BDC-CC and DG.

$$y = \frac{I_{nom} - x}{1+x} \tag{20}$$

Where N, x, I_{nom} and y represent the project's life span, inflation rate, nominal interest rate, and discount rate, respectively.

The annual replacement costs of microgrid components are computed as follows to determine their present value:

$$P_{V,REP} = \left(N_{BATT} \times C_{BATT,REP}\right) \times \sum_{b=1}^{N_r} \frac{(1+x)^{bN_c-1}}{(1+y)^{bN_c}} + \left(C_{DG,REP} \times \sum_{b=1}^{N_r} \frac{(1+x)^{bN_c-1}}{(1+y)^{bN_c}}\right) \tag{21}$$

Where $C_{BATT,REP}$ and $C_{DG,REP}$ represent the replacement cost of BATT and DG.

$$N_r = int\left(\frac{N - N_C}{N_C}\right) \tag{22}$$

Where N_C represent the life duration of each component, while N_r denotes the quantity of replacements necessary for the system components.

The following equation will be used to determine the annual fuel expense of the microgrid component:

$$P_{V,FUEL} = TAFCIL_{DG} \times \sum_{i=1}^{N} \frac{(1+x)^{i-1}}{(1+y)^{i}} \tag{23}$$

Where $TAFCIL_{DG}$ represent the total annual fuel consumption in liters of the DG.

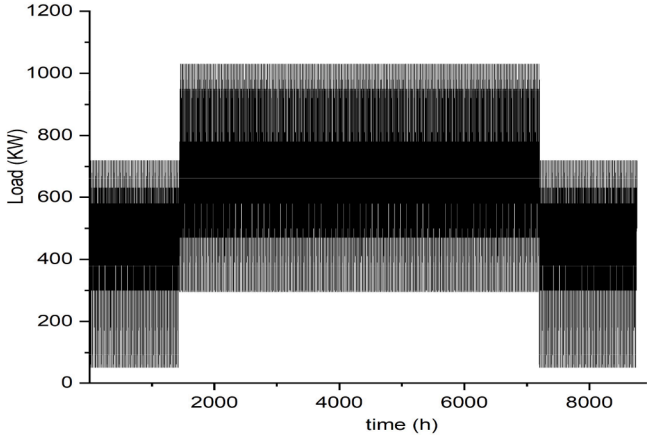

Fig. 8. Annual load demand.

4. Problem formulation

The objective function is defined based on the life cycle cost (LCC), cost of energy (COE), and constraints involved with the PV, WT, BESS, and DG. These factors will now be addressed in detail below:

4.1. Objective function

Life Cycle cost (LCC):

Minimize the LCC of the system while addressing the constraints with an LPSP of 0%. The LCC depend on four parameters: the number of PV panels (N_{PV}), wind turbines (N_{WT}), batteries (N_{BATT}) and diesel generator (N_{DG}).

$$min\ LCC(N_{PV},\ N_{WT},\ N_{BATT},\ N_{DG}) = \sum_{C=PV,WT,BATT,DG}^{min} (LCC)_C \tag{24}$$

Cost of Energy (COE):

One of the most important factors in assessing the economic feasibility of a microgrid is the COE, which includes the LCC, capital recovery factor (CRF), and electrical load (E_L).

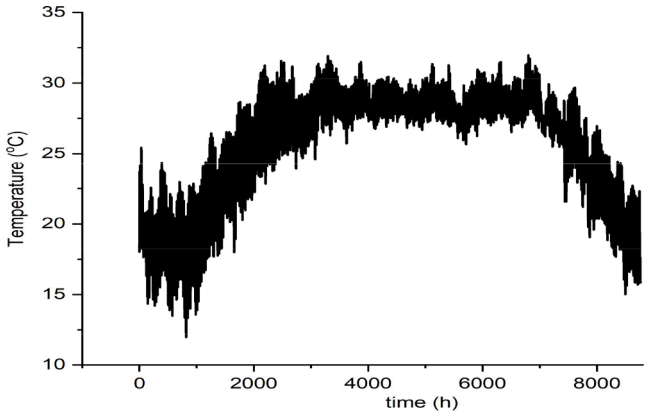

Fig. 9. Annual ambient temperature.

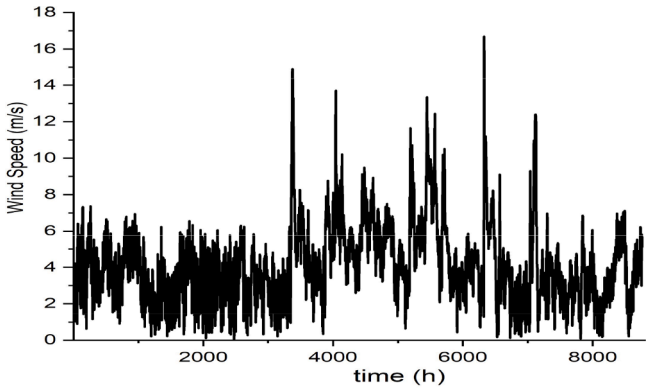

Fig. 11. Annual wind speed.

$$COE = \left(\frac{LCC}{\sum_{t=1}^{8760} E_L(t)}\right) \times CRF \tag{25}$$

4.2. Constraints

Upper and Lower bounds:

The study's lower bound is zero, and the upper bound is the maximum generation limit. Therefore, it remains subject to all constraints. Apply the following constraints to the remaining sources: solar, wind, battery, and diesel.

$$0 \le N_{PV} \le N_{PVmax} \tag{26}$$

$$0 \le N_{WT} \le N_{WTmax} \tag{27}$$

$$0 \le N_{BATT} \le N_{BATTmax} \tag{28}$$

$$0 \le N_{DG} \le N_{DGmax} \tag{29}$$

Battery Energy Storage limits:

The battery bank will store or discharge a certain amount of energy, which the following constrain [40]:

$$E_{BATTmin} \le E_{BATT}(t) \le E_{BATTmax} \tag{30}$$

The maximum and minimum limits for battery energy stored are calculated as follows:

$$E_{BATTmax} = \left(\frac{N_{BATT} \times V_{BATT} \times S_{BATT}}{1000}\right) \times SOC_{max-bat} \tag{31}$$

$$E_{BATTmin} = \left(\frac{N_{BATT} \times V_{BATT} \times S_{BATT}}{1000}\right) \times SOC_{min-bat} \tag{32}$$

Where V_{BATT} and S_{BATT} represent the voltage and rated capacity (Ah) of the battery.

The minimum and maximum limits for the state of charge (*SOC*) of the battery are calculated as follows:

$$SOC_{min-bat} = 1 - DOD \tag{33}$$

$$SOC_{max-bat} = SOC_{min-bat} + DOD \tag{34}$$

Where DOD represent the depth of discharge.

Diesel Generator (DG) Limit:

The study determines that the minimum load necessary for DG operation is 50% of its rated capacity. Consequently, the DG will operate in a simulation once it complies with the specified limits outlined below [41]:

$$\frac{E_L(t)}{\eta_{conv}} \ge P_{DG,\,rat} \times \Delta t \tag{35}$$

Power Reliability Index:

The reliability index for energy relates to its consistent ability to provide a dependable power supply under particular conditions. The evaluation of microgrid power reliability entails the computation of the loss of power supply probability (LPSP), which denotes the likelihood of power supply failure. The hourly energy demand and power supply loss (LPS) are utilized to derive the calculation [42]:

$$LPS(t) = \frac{E_L(t)}{\eta_{conv}} - E_G(t) - [(1-\sigma) \times E_{BATT}(t-1) - E_{Batt-min}] \times \eta_{rbatt} \tag{36}$$

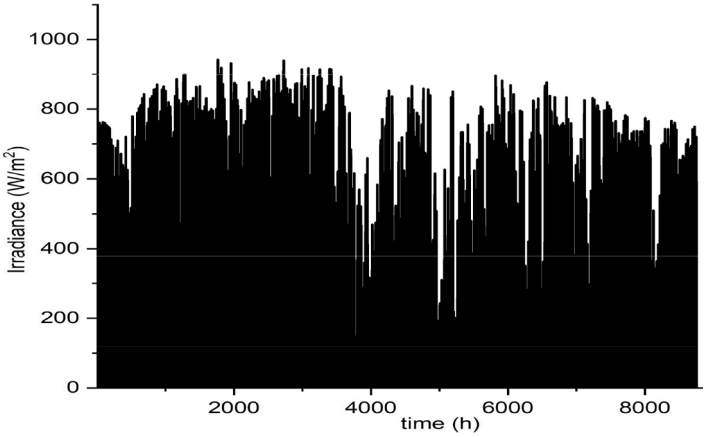

Fig. 10. Annual solar irradiance.

Table 3
Economic and technical specifications of PV, WT and DG parameters.

Parameters	Value	Parameters	Value
Project lifetime	25 years	Cut-out speed of WT	21 m/s
Nominal interest rate	8%	Rated speed of WT	11 m/s
Inflation rate	3%	Capital cost of WT	$2500
Rated power of PV Panel [43]	0.25kWp	AO&M cost of WT	$75
Lifetime of PV Panel	25 years	DG (Company: Mitsubishi, Model No: ST-M1600GF) [49]	2000 KVA
Capital cost of PV Panel	$250.00	C&R of DG	$200,000
AO&M cost of PV Panel	$6.25	Diesel Price	$0.97
Rated power of WT [43]	1kW	Rated power of BDC-CC [40]	2000kW
Lifetime of WT	25 years	Lifetime of converter	10 years
Hub height of WT	20 m	Capital cost of converter	$172,800
Reference height of WT	10 m	AO&M cost of converter	2.5% of CC
Cut-in speed of WT	2.5 m/s	Efficiency of converter	95%

Table 4
Economic and technical specifications of the batteries.

Battery Type	Lead Acid ($PbSO_4$)	Lithium Iron Phosphate ($LiFePO_4$)	Nickel Iron (Ni-Fe)
Manufacturer	Trojan [50]	Victron [51]	Iron Edison [52]
Model	SSIG 06 490	LFP-12.8/200-a	TN 1000
Round trip efficiency (ηrbat)	85%	92%	80%
Lifespan in years	3 years @70% DOD	9 years @70% DOD	30 years @70% DOD
Self-discharge rate (%/day) (σ)	0.30%	0.20%	1.00%
Capital cost (CC)	$410	$3317	$1057
Annual O&M cost	2.5% of CC	No maintenance	2% of CC
Operating temperature	−20 °C to +45 °C	−20 °C to +50 °C	−30° C to +60° C
Cycle life of the batteries	800 cycles	3000 cycles	11,000 cycles
Operating temperature	−20 °C to +45 °C	300Ah	1000Ah

$$LPSP = \frac{\sum_{t=1}^{T} LPS(t)}{\sum_{t=1}^{T} E_L(t)} \tag{37}$$

5. Pelican optimization algorithm (POA)

Dehghani and Trojovsk [34] developed the POA in 2022, drawing inspiration from nature. The reasons for selecting the POA technique are that it outperforms existing techniques by efficiently balancing the exploration and exploitation phases, resulting in better and more competitive performance and fast convergence speed [48]. The POA method is population-based; pelicans are included. In algorithms based on populations, each element signifies a prospective solution. All population members set forth proposed values for the variables linked to the optimization problem based on their respective positions in the search space. Eq. (38) randomly populates the population, constrained by the problem's upper and lower bounds.

$$X_{ij} = l_j + rand.\left(u_j - l_j\right),\ i = 1.2, \ldots, N,\ j = 1, 2, \ldots,\ m, \tag{38}$$

Where *xi, j* represents the j^{th} variable in the i^{th} feasible solution. The population size is denoted by the symbol *N*. The quantity of variables representing problems is denoted as *m*. The random number "r*and*" is inside the interval [0, 1]. L_j represents the j^{th} lower bound and j^{th} upper bound of the problem variables, denoted as u_j.

$$X = \begin{bmatrix} X_1 \\ \vdots \\ X_i \\ \vdots \\ X_N \end{bmatrix}_{N\times m} = \begin{bmatrix} x_{1,1} & \cdots & x_{1,j} & \cdots & x_{1,m} \\ \vdots & \ddots & \vdots & \iddots & \vdots \\ x_{i,1} & \cdots & x_{i,j} & \cdots & x_{i,m} \\ \vdots & \iddots & \vdots & \ddots & \vdots \\ x_{N,1} & \cdots & x_{N,j} & \cdots & x_{N,m} \end{bmatrix}_{N\times m} \tag{39}$$

Where *X* is the matrix that represents the pelican population, and X*i* represents the i^{th} individual pelican.

As every individual in the POA population is a pelican, this may present an acceptable resolution. Thus, evaluating the problem's objective function is feasible by analyzing every possible solution. Eq. (40) and a vector referred to as the objective function vector are utilized to ascertain the values of the objective function.

$$F = \begin{bmatrix} F_1 \\ \vdots \\ F_i \\ \vdots \\ F_N \end{bmatrix}_{N\times 1} = \begin{bmatrix} F(X_1) \\ \vdots \\ F(X_i) \\ \vdots \\ F(X_N) \end{bmatrix}_{N\times 1} \tag{40}$$

The pelican's hunting process consists of two distinct phases, which are referred to as exploitation and exploration. Exploration entails movement in the direction of the prey, as opposed to exploitation, which requires flying on the water's surface. During the initial phase, pelicans identify and go towards their prey. The random generation of the location of the prey enhances POA's exploration efficiency. The initial phase is mathematically represented by Eq. (41).

Table 5
Optimization results for sizing of the microgrid components.

Configuration	Quantity	GA	PSO	MFOA	WOA	GWO	**Proposed POA**
PV/WT/LA/DG	Number of PV (NPV)	8186	9854	8446	8112	9180	**8621**
	Number of WT (NWT)	10	10	16	9	10	**10**
	Number of batteries (NB)	6590	5464	5831	6173	5919	**6298**
	Total annual fuel consumption in liter (TAFCIL)	293	293	3535	9303	293	**7283**
PV/WT/Li-ion/DG	Number of PV (NPV)	11,205	11,205	11,345	11,210	11,200	**11,190**
	Number of WT (NWT)	10	10	6	11	14	**17**
	Number of batteries (NB)	3413	3413	3378	3357	3380	**3365**
	Total annual fuel consumption in liter (TAFCIL)	1752	1751	1270	1878	1749	**2100**
PV/WT/Ni-Fe/DG	Number of PV (NPV)	11,206	11,205	9925	11,208	7519	**7494**
	Number of WT (NWT)	11	10	18	12	13	**15**
	Number of batteries (NB)	4458	4458	5145	4380	5680	**5725**
	Total annual fuel consumption in liter (TAFCIL)	1751	1751	4560	1930	20,425	**23,125**

Table 6
Optimized results for LCC and COE for different configuration of microgrid components.

Configuration	Cost	GA	PSO	MFOA	WOA	GWO	**Proposed POA**
PV/WT/LA/DG	LCC ($)	8,424,687	8,395,820	8,370,410	8,402,974	8,343,961	**8,334,901**
	COE ($/kWh)	0.1092	0.1088	0.1085	0.1089	0.1082	**0.1080**
PV/WT/Li-ion/DG	LCC ($)	25,806,669	25,724,017	25,711,682	25,745,936	25,706,042	**25,645,632**
	COE ($/kWh)	0.3346	0.3335	0.3333	0.3337	0.3331	**0.3323**
PV/WT/Ni-Fe/DG	LCC ($)	12,312,606	12,229,955	12,192,940	12,280,376	12,038,965	**11,926,161**
	COE ($/kWh)	0.1596	0.1584	0.1579	0.1590	0.1561	**0.1546**

$$x_{i,j}^{P_1} = \begin{cases} x_{i,j} + rand.\left(p_j - l.x_{i,j}\right), & F_p^1 < F_i; \\ x_{i,j} + rand.\left(x_{i,j} - p_j\right), & else, \end{cases} \tag{41}$$

Where F_p & $x_{i,j}^{P_1}$ represent the prey's objective function value, a random number l equal to 1, or 2, and the i^{th} pelican's new status in the j^{th} dimension based on the first phase. A new position of a pelican becomes permissible within the bounds of POA if the objective function value increases at that particular location. By employing this methodology, known as "effective updating," the algorithm avoids its progression through suboptimal regions. From a mathematical standpoint,

$$X_i = \begin{cases} X_i^{P_1}, & F_i^{P_1} < F_i; \\ X_i, & else, \end{cases} \tag{42}$$

Where $X_i^{\mathbb{P}}$ denotes the updated status of the i^{th} pelican, whereas $F_i^{\mathbb{P}}$ represents the value of the pelican's objective function calculated during the initial phase.

During the second phase, pelicans employ the water's surface to generate upward propulsion for the fish by extending their wings, subsequently trapping the prey in their throat bag. Consequently, pelicans can catch a greater quantity of fish. The exploitation potential of POA is enhanced during this phase as the algorithm approaches more optimal solutions in the hunting zone. The hunting procedure is formulated as follows:

$$x_{i,j}^{P_2} = x_{i,j} + R.\left(1 - \frac{t}{T}\right).(2.rand - 1).x_{i,j} \tag{43}$$

Where $x_{i,j}^{P_2}$ denotes the updated state of the i^{th} pelicans in the J^{th} dimension during the second phase. The constant R equals 0.2 and $R.(1-t/T)$ is an expression using t and T variables. The neighborhood radius of $x_{i,j}$ is determined by the iteration counter t and the maximum number of iterations T. At this point, the approval or rejection of the newest pelican position has been determined through efficient updating, as illustrated in Eq. (44):

$$X_i = \begin{cases} X_i^{P_2}, & F_i^{P_2} < F_i; \\ X_i, & else, \end{cases} \tag{44}$$

Where $X_i^{P_2}$ indicates the updated status of the i^{th} pelican, and denotes the objective function value of the pelican. This next iteration begins once every member of the population has been updated. Throughout this process, a series of operations guided by Eqs. (41–44) are repeated until the execution is finished. The process of POA is illustrated in the flowchart and pseudocode are provided in Fig. 5 and 6.

5.1. Proposed solution

The proposed solution applied POA to determine the most efficient sizing for the microgrid, as depicted in Fig. 7. At first, the particular details of the PV, WT, DG, battery, converter, and load were figured out. Meteorological information about the installation site has been recorded, which includes longitude, latitude, wind speed, solar radiation, and ambient temperature. Also,

EMS incorporates microgrids that manage power flow among numerous system elements. Each probable solution, which includes the number of PV panels (N_{PV}), the number of wind turbines (N_{WT}), and the number of batteries (N_B), undergoes the POA steps. The LPSP is computed to evaluate the proposed solution's reliability. A convergence of the LPSP to one signifies that the load is unsatisfied, leaving the solution unfeasible. When this occurs, the procedure is iteratively applied to the following feasible solution from the population. The RESs produced can meet the capacity requirements once the LPSP reaches zero. Through the iterative repetition of the procedures, the iterations are ultimately concluded, yielding an accurate microgrid capable of fulfilling the load demands for the system's life.

Table 7
Amount of GHG emission for different configuration of microgrid components.

Configuration	Emission	GA	PSO	MFOA	WOA	GWO	**Proposed POA**
PV/WT/LA/DG	CO_2 (kgs/year)	789	789	9545	25,120	789	**19,664**
PV/WT/Li-ion/DG	CO_2 (kgs/year)	4730	4729	3429	5071	4723	**5670**
PV/WT/Ni-Fe/DG	CO_2 (kgs/year)	4729	4729	12,312	5211	55,148	**62,437**

6. Results and discussion

The study implements the microgrid system's optimal sizing utilizing MATLAB, considering GA, PSO, GWO, and the proposed approach POA. The microgrid system comprises PV, WT, DG, and BESS. The case study area is Kutubdia Island of Bangladesh, located at 21.8167°S and 91.8583°E. Initially, input data, such as wind speed, solar irradiance, and load demand data, were collected. The historical data was sourced from the National Aeronautics and Space Administration (NASA). The island microgrid undergoes fluctuations in its hourly load requirement, which can vary from 50 – 1100 kW. Fig. 8 illustrates the yearly load curve for a typical year. Fig. 9–11 display the annual temperature, irradiance, and wind speed respectively. The island microgrid's components are vulnerable to the effects of natural disasters. To guarantee the system's dependability, it is necessary to consider components with suitable rated capacity to prevent outages resulting from equipment failure. The economic and technical specifications of the PV, WT, DG and battery parameters are presented in Table 3 and 4.

The optimal solutions for the three configurations of microgrid generated by the six algorithms are displayed in Tables 5, 6, and 7. The default parameters of the algorithms, GA, PSO, MFOA, WOA GWO, and the proposed approach, POA, are run with a maximum number of iterations of 100 and a maximum population size of 100. Each solution has an LPSP value of 0 %. All the results presented in the tables show that LA battery-based configuration (PV/WT/LA/DG) is the best among all the three configurations. In Table 5, the optimal number of PV panels, wind turbines, batteries, and diesel generators are presented for different configurations of microgrid to achieve optimal sizing. The proposed POA approach predicts 8621 PV panels, 10 wind turbines, 6298 batteries, and 7283 liters of DG annually are required to design an economically feasible microgrid compared to other optimization techniques. The optimal results for LCC and COE are presented in Table 6 for all the three configurations of microgrid. POA approach obtained PV/WT/LA/DG configuration has a minimum LCC and the system's lowest COE which are $ 8,334,901 and 0.1080 $/kWh. Table 7 provides the GHG emission results for microgrid different configurations obtained by different optimization methods. It is observed that for the proposed POA approach, the total GHG emission is 19,664 kgs/year for microgrids PV/WT/LA/DG configuration. The charging and discharging process for the

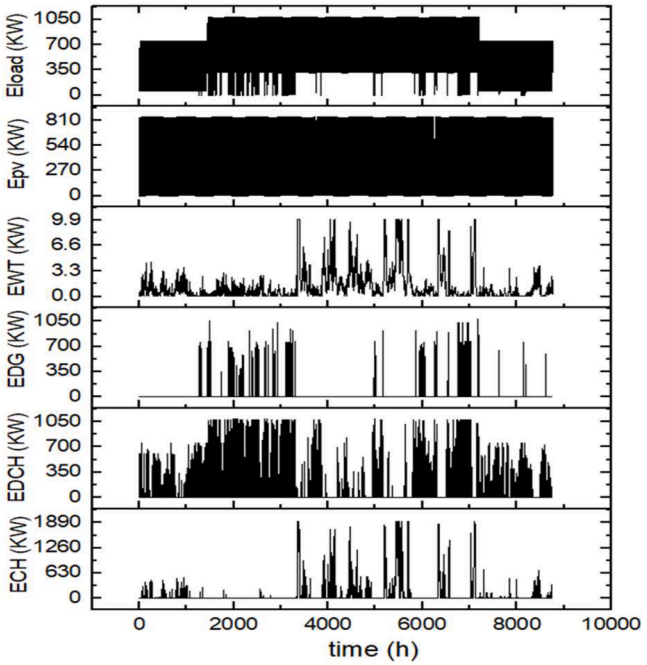

Fig. 12. Annual electricity generation of microgrid.

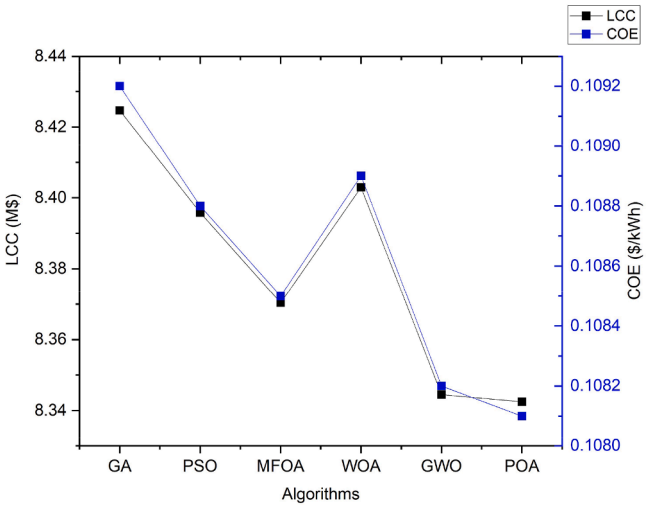

Fig. 13. LCC and COE variation for different algorithms.

LA battery bank in response to load demand, along with the annual energy generation from PV, WT, and DG, are depicted in Fig. 12. Comparing the proposed method to different methods for determining the variation of LCC and COE is shown in Fig. 13. The proposed approach has a lower LCC and COE than other methods. The GWO method show an increase of 0.1 %, the WOA method show a rise of 0,82 %, the MFOA method show an increase of 0.43 %, the PSO method shows a rise of 0.7 %, and the GA method shows an increase of 1 %. Fig. 14 and 15 show the energy output graphs for the base case in the summer and winter seasons for one month (May and December), respectively. According to the figure, it is observed that from morning 7 a.m. to evening 5 p.m. in summer, and from morning 9 a.m. to evening 4 p.m. in winter, the PV and WT supply the estimated load demand. The excess energy generated is used to charge the batteries. The batteries and WT supply the total load demand from 6 a.m. to early morning, repeating this cycle for the summer and winter seasons.

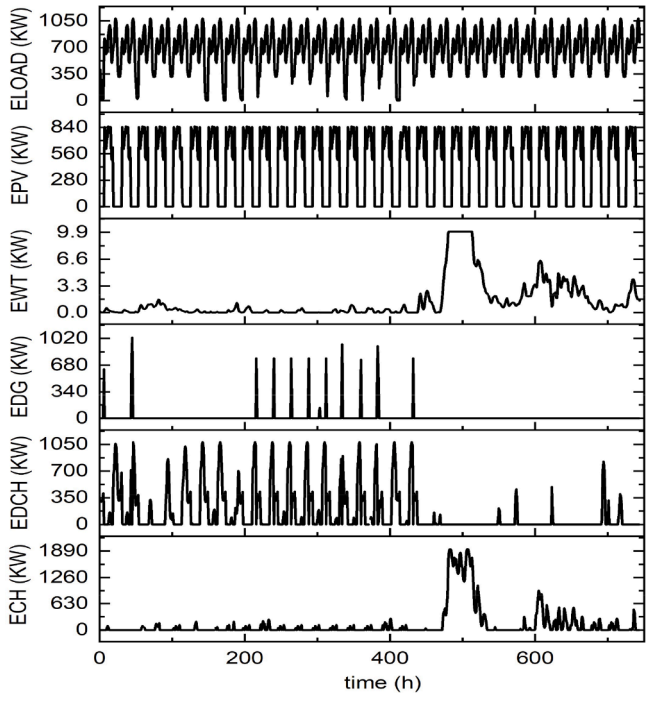

Fig. 14. Energy outputs of islanded microgrid during summer season in May month.

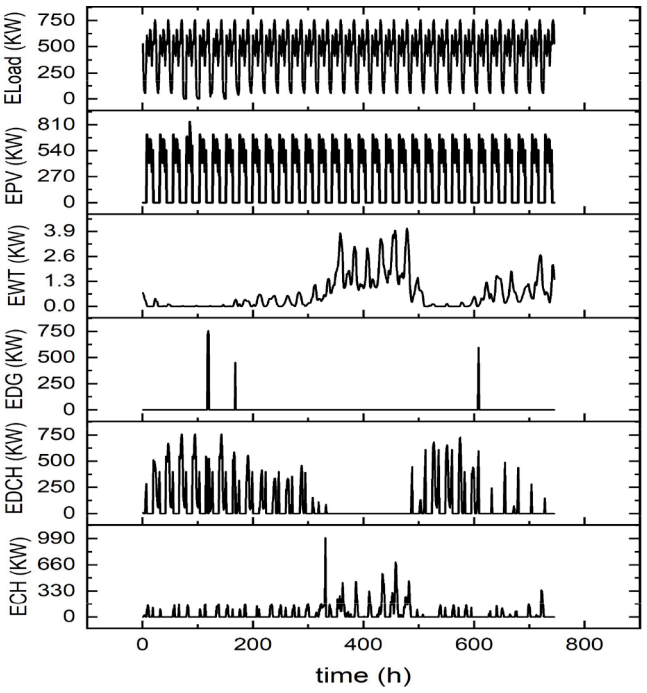

Fig. 15. Energy outputs of islanded microgrid during winter season in December month.

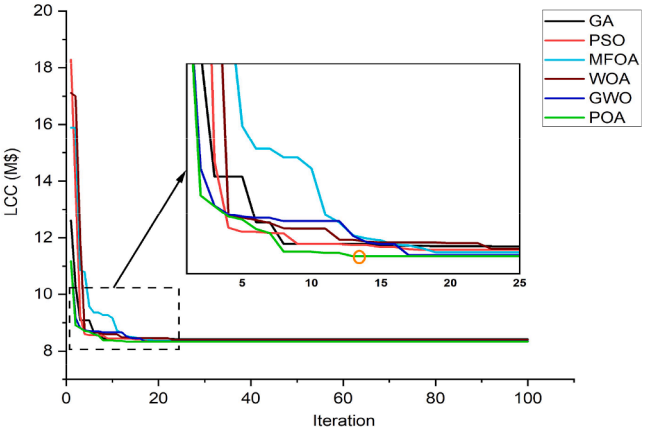

Fig. 16. Convergence curve of the LA battery based microgrid for different algorithms.

6.1. Effect of LA/Li-ion/Ni-Fe battery technology

The LA battery-based microgrid shows the lowest LCC and COE, equal to $8,334,901 and 0.1080$/KWh, as presented in Table 4. This study's base case represents an optimal value in comparison to different configurations of battery-based microgrids. The Li-ion-powered microgrid has an LCC and COE of $25,645,632 and 0.3323$/KWh, respectively, approximately 207 % greater than the base case. The Ni-Fe battery-powered microgrid exhibits an LCC of $11,926,161 and a COE of 0.1546 $/kWh, roughly 43% greater than the base.

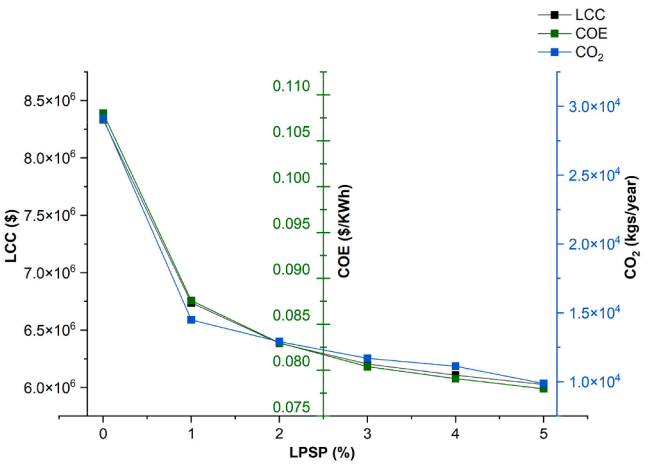

Fig. 17. Variation in corresponding components LCC, COE and CO_2 at various LPSP values.

6.2. Convergence speed

The convergence curve of each algorithm for the LA-based microgrid is illustrated in Fig. 16. The proposed method reached the minimum LCC at the 20th, 18th, 19th, 23rd, 17th, and **13th** (orange circle) iterations, respectively, through the convergence of GA, PSO, MFOA, WOA, GWO, and POA algorithms to the optimal value of LCC.

6.3. Effect of reliability index (LPSP)

As mentioned in Section 6.1, the LA-based microgrid using the proposed technique is the best configuration at 0% LPSP. Further analysis was conducted using the proposed POA approach at various reliability index values to identify optimal values. The optimized value of the proposed technique based on the LA microgrid for different reliability index (LPSP) values is shown in Table 8. A significant difference has been noted between the LPSP values of 0 % and 1 %. An analysis of the data shows a significant reduction in the quantity of PV panels (8621 – 7296) and batteries (6298 – 4458), respectively. However, the number of WTs remains unchanged across all values. Moreover, the LCC and COE values have each been lowered by 29 %. LPSP, or Loss of Power Supply Hours, comprises just 88 out of 8760 hours, or 1 % of the total. As shown in Fig. 17, the corresponding values for LPSP increase while those for the remaining parameters decrease.

6.4. Sensitivity analysis

A sensitivity analysis evaluated the optimal configuration to determine the effect of the interest rate input parameter by varying LCC, COE, and CO_2. The study involved adjusting the interest rate by ±20%. The optimum configuration is the base case, with an LCC of $8334,901 and a COE of 0.1080 $/kWh. Table 9 presents the optimum design outcome

Table 8
Different reliability index (LPSP) values within the optimal configuration.

Configuration	Quantity & Cost	LPSP (0%)	LPSP (1%)	LPSP (2%)	LPSP (3%)	LPSP (4%)	LPSP (5%)
PV/WT/LA/DG	NPV	8621	7296	6766	6536	6418	6339
	NWT	10	10	10	10	10	10
	NB	6298	4458	3843	3707	3576	3462
	CO_2 (kgs/year)	19,664	14,502	12,913	11,702	11,139	9884
	LCC ($)	8,334,901	6,738,262	6,386,766	6,205,964	6,107,525	6,026,669
	COE ($/kWh)	0.1080	0.0876	0.0830	0.0804	0.0791	0.0780

Table 9
Variation of interest rates within the optimal configuration.

Components	-20% of base case	-10% of base case	Base case	+10% of the base case	+20% of base case
Interest rate	6.4%	7.2%	**8%**	8.8%	9.6%
LCC	8,255,859	8,306,619	**8,334,901**	8,413,215	8,496,312
COE	0.1069	0.1076	**0.1080**	0.1090	0.1101
CO_2	22,829	26,000	**19,664**	33,416	37,707

Table 10
Comparison among POA and other approaches used for techno-economic analysis at Kutubdia Island.

Ref.	Sources used in microgrid	Techniques	LCC	COE	CO_2 emission
[35]	PV/WT/DG/ BESS	HOMER	×	0.235 $/kWh	522,110 (kg/yr)
[44]	PV/DG/BESS	HOMER	×	×	2649,251 (kg/yr)
[45]	PV/WT/DG/ BESS	NSGA	×	0.2 $/kWh	62,075 (kg/ yr)
[46]	PV/WT/DG	HOMER	×	0.4 $/kWh	132,786 (kg/yr)
[47]	PV/ Biogas/ DG	HOMER	×	0.42 $/kWh	×
Proposed work	**PV/WT/DG/ BESS**	**POA**	√	**0.1080 $/kWh**	**19,664 (kg/yr)**

when varying the interest rate. A rise in the interest rate on the system from 10 % to 20 % of its base case has been found to result in an increase in the system LCC and COE from 0.9 % – 1.9 %, and CO_2 emission from 13 % – 23 % compared to the base case. In the same way, a reduction in the system's interest rate from 10 % –20 % relative to its base case reduces the LCC and COE by 0.4 % – 1 %, respectively, and decreases CO_2 emissions by 12 % and 27 % compared to the base case. The effectiveness of the system is greatly affected by the interest rate.

6.5. Comparative analysis

Table 10 presents a comparative study that illustrates the performance of the developed system at Kutubdia Island in previous works. Several studies have been conducted on the design of a microgrid supplied by RESs for Kutubdia Island. LCC has not been taken into consideration in majority the studies. The COE and CO_2 emissions for the proposed approach are 0.1080$/kWh and 19,664 kg/yr, which is less than the previous works. Furthermore, the proposed approach, POA-based performance used for microgrids optimal sizing has been compared with optimization techniques such as GA [12], PSO [13], MFOA [14], ACO [15], WOA [17], GOA [18], FOA [19], GWO [20], and HHO [21] based on values of LCC, COE and amount of CO_2 emission which is presented in Table 11. From the table it is observed that proposed POA optimization technique has outperformed the performance of all existing methods which have been used for optimization of different microgrid around the world.

Table 11
Comparison among optimization methods used for optimal sizing of different microgrid systems.

Ref.	Techniques	LCC	COE	CO_2 emission
[17]	GA	×	×	104,323.10 (kg/yr)
[18]	PSO	×	0.10006 $/kWh	272,811.16(kg/yr)
[19]	MFOA	×	0.60 $/kWh	×
[20]	ACO	×	1.082 $/kWh	11,833 (kg/yr)
[22]	WOA	×	0.1986 $/kWh	×
[23]	GOA	×	×	×
[24]	FOA	×	0.085 $/kWh	×
[25]	GWO	×	0.12 $/kWh	×
[26]	HHO	×	0.20 $/kWh	×
Proposed work	**POA**	√	**0.1080 $/kWh**	**19,664 (kg/yr)**

7. Conclusion

An optimization approach, POA, is proposed to determine the optimal sizing of microgrid components for Kutubdia Island in Bangladesh, where the expansion of the distribution network is not feasible while attaining minimum LCC and COE. Furthermore, a study on the selection of three battery technologies has been conducted on LA, Li-ion, and Ni-Fe for continuous power supply. The proposed POA gives the optimal configuration of the island microgrid with optimal LCC and COE values compared to other optimization techniques, GA, PSO, GWO, MFOA, and WOA. LA battery-based microgrid provided the optimal LCC and COE, amounting to $8,334,901 and 0.1080$/KWh, respectively, as determined by the results. The Li-ion-powered microgrid exhibits a COE of 0.3323 $/KWh and an LCC of $25,645,632, approximately 67.5 % greater than the optimal configuration. The LCC and COE of the Ni-Fe battery-powered microgrid are $11,926,161 and 0.1546 $/kWh, which are 30% greater than the optimal configuration. Optimal configurations are determined across a range of LPSP values between 0% and 5 %. Despite a slight reduction in power supply hours, it is noted that the optimal configuration yields superior outcomes in terms of LCC and COE. Additionally, a sensitivity analysis was performed by regulating interest rates. It has been observed that interest rates have a greater impact on system effectiveness. Finally, a comparative study based on LCC, COE, and CO_2 emissions with previous works was performed, demonstrating that the proposed POA provides superior results compared to the previous works. The future scope involves the development of a multi-objective algorithm based on POA to solve continuous multi-objective problems. Additionally, effective planning can reduce peak load demands by implementing energy conservation management and rescheduling off-peak load demand periods. Implementing this strategy may result in a substantial decrease in investment expenses.

CRediT authorship contribution statement

Abidur Rahman Sagor: Writing – original draft, Software, Methodology, Formal analysis, Data curation, Conceptualization. **Md. Rifat Hazari:** Writing – original draft, Visualization, Validation, Supervision, Methodology, Formal analysis, Data curation, Conceptualization. **Shameem Ahmad:** Writing – original draft, Supervision, Software, Methodology, Data curation, Conceptualization. **Emanuele Ogliari:** Writing – review & editing, Validation, Investigation. **Chowdhury Akram Hossain:** Writing – review & editing, Methodology, Investigation. **Effat Jahan:** Writing – review & editing, Validation, Investigation. **Mohammad Abdul Mannan:** Writing – review & editing, Visualization, Validation, Investigation.

Declaration of competing interest

The authors declare that they have no known competing financial interests or personal relationships that could have appeared to influence the work reported in this paper.

The author is an Editorial Board Member/Editor-in-Chief/Associate Editor/Guest Editor for *Electric Power Systems Research* and was not involved in the editorial review or the decision to publish this article.

Data availability

The data used for this research are included within the manuscript.

References

[1] A. Naderipour, H. Saboori, H. Mehrjerdi, S. Jadid, Z. Abdul-Malek, Sustainable and reliable hybrid AC/DC microgrid planning considering technology choice of equipment, Sustain. Energy Grids Netw., 23 (2020) 100386.

[2] T. Stewart, Dealing with uncertainties in MCDA, Multiple criteria decision analysis: State of the art surveys (2005) 445–466.

[3] Duong, M.Q., Tran, N.T.N., & Hossain, C.A. (2019, January). The Impact of Photovoltaic Penetration with Real Case: ThuaThienHue–Vietnamese Grid. In 2019 International Conference on Robotics, Electrical and Signal Processing Techniques (ICREST) (pp. 682–686). IEEE.

[4] R.J. Zedalis, International energy law, Int. Energy Law (2017), https://doi.org/10.4324/9781315252056.

[5] M.F. Zia, E. Elbouchikhi, M. Benbouzid, Microgrids energy management systems: A critical review on methods, solutions, and prospects, Appl. Energy 222 (2018) 1033–1055.

[6] M.A. Abdulgalil, M. Khalid, F. Alismail, Optimal sizing of battery energy storage for a grid-connected microgrid subjected to wind uncertainties, Energies. (Basel) 12 (12) (2019) 2412.

[7] T.H. Faria, Shamim Kaiser, Hossian M, A. C, M. Mahmud, S. Al Mamun, C Chakraborty, Smart city technologies for next generation healthcare. Data-Driven Mining, Learning and Analytics for Secured Smart Cities: Trends and Advances, Springer International Publishing, Cham, 2021, pp. 253–274.

[8] E. Beshr, Comparative study of adding PV/wind energy systems to autonomus micro grid, in: 2013 3rd International Conference on Electric Power and Energy Conversion Systems, IEEE, 2013, pp. 1–6.

[9] V. Krepl, H.I. Shaheen, G. Fandi, L. Smutka, Z. Muller, J. Tlustý, T. Husein, S. Ghanem, The role of renewable energies in the sustainable development of post-crisis electrical power sectors reconstruction, Energies. (Basel) 13 (23) (2020) 6326.

[10] Hasan, M.M., Chowdhury, N., Hossain, C.A., & Longo, M. (2019). State of art on possibility & optimization of solar PV-wind hybrid system. In 2019 International Conference on Robotics, Electrical and Signal Processing Techniques (ICREST) (pp. 598–601). IEEE.

[11] L.A.D.S. Ribeiro, O.R. Saavedra, S.L. Lima, J.G. de Matos, G. Bonan, Making isolated renewable energy systems more reliable, Renew. Energy 45 (2012) 221–231.

[12] D. Wu, X. Ma, S. Huang, T. Fu, P. Balducci, Stochastic optimal sizing of distributed energy resources for a cost-effective and resilient microgrid, Energy 198 (2020) 117284.

[13] M. Zishan, C. Hossain, M. Mohamed, S. Sharun, The scenario of e-health systems in developing countries (Bangladesh and Malaysia), Int. J. Recent Technol. Eng. (IJRTE) 8 (2019) 1138–1143.

[14] M. Fathi, R. Khezri, A. Yazdani, A. Mahmoudi, Comparative study of metaheuristic algorithms for optimal sizing of standalone microgrids in a remote area community, Neural Comput. Appl. 34 (7) (2022) 5181–5199.

[15] M. Thirunavukkarasu, Y. Sawle, H. Lala, A comprehensive review on optimization of hybrid renewable energy systems using various optimization techniques, Renew. Sustain. Energy Rev. 176 (2023) 113192.

[16] D. Debnath, C.A. Hossain, R. Islam, M. Tarique, I.K. Dutta, Minimizing shadowing effects on mobile ad hoc networks, J. Sel. Areas commun. 1 (10) (2011) 46–51.

[17] F.A. Alturki, A.A. Al-Shamma'a, H.M. Farh, K. AlSharabi, Optimal sizing of autonomous hybrid energy system using supply-demand-based optimization algorithm, Int. J. Energy Res. 45 (1) (2021) 605–625.

[18] A.Q. Mohammed, K.A. Al-Anbarri, R.M. Hannun, Using PSO to find optimal sizing of PV-BS and diesel generator, J. eng. sustain. dev. 25 (3) (2021) 51–59.

[19] J. Bandopadhyay, P.K. Roy, Application of hybrid multi-objective moth flame optimization technique for optimal performance of hybrid micro-grid system, Appl. Soft. Comput. 95 (2020) 106487.

[20] F.K. Abo-Elyousr, A. Elnozahy, Bi-objective economic feasibility of hybrid micro-grid systems with multiple fuel options for islanded areas in Egypt, Renew. Energy 128 (2018) 37–56.

[21] D.K. Geleta, M.S. Manshahia, Artificial bee colony-based optimization of hybrid wind and solar renewable energy system. Handbook of Research On Energy-Saving Technologies For Environmentally-Friendly Agricultural Development, IGI Global, 2020, pp. 429–453.

[22] A.A.Z. Diab, H.M. Sultan, I.S. Mohamed, O.N. Kuznetsov, T.D. Do, Application of different optimization algorithms for optimal sizing of PV/wind/diesel/battery storage stand-alone hybrid microgrid, IEEe Access. 7 (2019) 119223–119245.

[23] A.A. Al-Shamma'a, H.M. Farh, A.A. Alkuhayli, A.M. Noman, A.M. Abdurraqeeb, Grasshopper Optimization Algorithm for Optimal Sizing of a Stand-Alone Hybrid Energy System, in: 2022 IEEE 16th International Conference on Compatibility, Power Electronics, and Power Engineering, 2022, pp. 1–6.

[24] S. Sanajaoba, Optimal sizing of off-grid hybrid energy system based on minimum cost of energy and reliability criteria using firefly algorithm, Solar Energy 188 (2019) 655–666.

[25] R. Kaur, V. Krishnasamy, N.K. Kandasamy, S. Kumar, Discrete multiobjective grey wolf algorithm based optimal sizing and sensitivity analysis of PV-wind-battery system for rural telecom towers, IEEe Syst. J. 14 (1) (2019) 729–737.

[26] İ. Çetinbaş, B. Tamyürek, M. Demirtaş, Sizing optimization and design of an autonomous AC microgrid for commercial loads using Harris Hawks Optimization algorithm, Energy Convers. Manage 245 (2021) 114562.

[27] P.P. Kumar, R.P. Saini, Optimization of an off-grid integrated hybrid renewable energy system with different battery technologies for rural electrification in India, J. Energy Storage 32 (2020) 101912.

[28] M.E. Sallam, M.A. Attia, A.Y. Abdelaziz, M.A. Sameh, A.H. Yakout, Optimal Sizing of Different Energy Sources in an Isolated Hybrid Microgrid Using Turbulent Flow Water-Based Optimization Algorithm, IEEe Access. 10 (2022) 61922–61936.

[29] D. Yang, C. Jiang, G. Cai, N. Huang, Optimal sizing of a wind/solar/battery/diesel hybrid microgrid based on typical scenarios considering meteorological variability, IET Renew. Power Gener. 13 (9) (2019) 1446–1455.

[30] A. Khan, N. Javaid, Jaya learning-based optimization for optimal sizing of stand-alone photovoltaic, wind turbine, and battery systems, Eng. 6 (7) (2020) 812–826.

[31] W. Cai, X. Li, A. Maleki, F. Pourfayaz, M.A. Rosen, M.A. Nazari, D.T. Bui, Optimal sizing and location based on economic parameters for an off-grid application of a hybrid system with photovoltaic, battery and diesel technology, Energy 201 (2020) 117480.

[32] M. Ristimäki, A. Säynäjoki, J. Heinonen, S. Junnila, Combining life cycle costing and life cycle assessment for an analysis of a new residential district energy system design, Energy 63 (2013) 168–179.

[33] L. Viktorsson, J.T. Heinonen, J.B. Skulason, R. Unnthorsson, A step towards the hydrogen economy—A life cycle cost analysis of a hydrogen refueling station, Energies. (Basel) 10 (6) (2017) 763.

[34] P. Trojovský, M. Dehghani, Pelican optimization algorithm: A novel nature-inspired algorithm for engineering applications, Sensors 22 (3) (2022) 855.

[35] M.A. Zaman, M.A. Razzak, Sustainable microgrid analysis for Kutubdia Island of Bangladesh, IEEe Access. 10 (2022) 37533–37556.

[36] A.L. Bukar, C.W. Tan, K.Y. Lau, Optimal sizing of an autonomous photovoltaic/wind/battery/diesel generator microgrid using grasshopper optimization algorithm, Solar Energy 188 (2019) 685–696.

[37] A.S.O. Ogunjuyigbe, T.R. Ayodele, O.A. Akinola, Optimal allocation and sizing of PV/Wind/Split-diesel/Battery hybrid energy system for minimizing life cycle cost, carbon emission and dump energy of remote residential building, Appl. Energy 171 (2016) 153–171.

[38] A.M. Patel, S.K. Singal, Optimal component selection of integrated renewable energy system for power generation in stand-alone applications, Energy 175 (2019) 481–504.

[39] K.F. Man, K.S. Tang, S. Kwong, Genetic algorithms: concepts and applications [in engineering design], IEEE Trans. Ind. Electron. 43 (5) (1996) 519–534.

[40] P Kumar, R.P Saini, Optimization of an off-grid integrated hybrid renewable energy system with various energy storage technologies using different dispatch strategies, Energy Sources, Part A: Recovery, Utilization, and Environ. Effects (2020) 1–30.

[41] T. Tu, G.P. Rajarathnam, A.M. Vassallo, Optimization of a stand-alone photovoltaic–wind–diesel–battery system with multi-layered demand scheduling, Renew. Energy 131 (2019) 333–347.

[42] P.P. Kumar, V. Suresh, M. Jasinski, Z. Leonowicz, Off-grid rural electrification in india using renewable energy resources and different battery technologies with a dynamic differential annealed optimization, Energies. (Basel) 14 (18) (2021) 5866.

[43] A. Bhatt, M.P. Sharma, R.P. Saini, Feasibility and sensitivity analysis of an off-grid micro hydro–photovoltaic–biomass and biogas–diesel–battery hybrid energy system for a remote area in Uttarakhand state, India. Renew. Sustain. Energy Rev. 61 (2016) 53–69.

[44] S.S. Yusuf, N.N. Mustafi, Design and simulation of an optimal mini-grid solar-diesel hybrid power generation system in a remote Bangladesh. International Journal of Smart Grids, ijSmartGrid 2 (1) (2018) 27–33.

[45] M.R. Islam, H. Akter, H.O.R. Howlader, T. Senjyu, Optimal sizing and techno-economic analysis of grid-independent hybrid energy system for sustained rural electrification in developing countries: A case study in Bangladesh, Energies. (Basel) 15 (17) (2022) 6381.

[46] S.K. Nandi, H.R. Ghosh, Techno-economical analysis of off-grid hybrid systems at Kutubdia Island, Bangladesh. Energy policy 38 (2) (2010) 976–980.

[47] S. Salehin, M.M. Ehsan, S. Noor, Sadrul Islam, K.M A, Modeling of an optimized hybrid energy system for Kutubdia Island, Bangladesh. Appl. Mech. Mater. 819 (2016) 518–522.

[48] A.R. Sagor, M.A. Talha, S. Ahmad, T. Ahmed, M.R. Alam, M.R. Hazari, G. M. Shafiullah, Pelican Optimization Algorithm-Based Proportional–Integral–Derivative Controller for Superior Frequency Regulation in Interconnected Multi-Area Power Generating System, Energies. (Basel) 17 (2024) 3308, 2024.

[49] "Mitsubishi heavy industries." https://engine-genset.mhi.com/.

[50] "Trojan Battery Company." https://www.trojanbattery.com/.

[51] Victron Energy Blue Power." https://www.victronenergy.com/batteries.

[52] "Iron Edison." https://ironedison.com/store.